

Experimental and numerical study on dynamic buckling of 304 stainless steel cylinders impacted by explosively driven flyer plates

Tetsuyuki Hiroe[†], Kazuhito Fujiwara, Hidehiro Hata, and Keisuke Sashima

Department of Advanced Mechanical Systems, Graduate School of Science and Technology, Kumamoto University, 2-39-1 Kurokami, Kumamoto 860-8555, JAPAN

[†] Corresponding address: hiroe@gpo.kumamoto-u.ac.jp

Received: February 29, 2008 Accepted: May 1, 2008

Abstract

In this study, smooth walled tubular specimens (L, Do, t: 100 × 34 × 3 mm) of 18Cr-8Ni stainless steel were vertically set on a steel support plate and impacted at the top side vertically or axially by circular flyer plates (D, h: 80 × 20 mm) of the same material. The direct explosive driver was a slab-like installed powder PETN (charged density: 0.90-0.95 × 10³ kg·m⁻³, height variations: 10, 15 and 20 mm) initiated by simultaneous explosion of paralleled fine copper wire rows placed over the entire outer surface using a discharge current from a high-voltage capacitor bank.

All the tested cylinders impacted at the estimated velocities of around 80, 92 and 120 m·s⁻¹ were locally buckled and plastically deformed mainly near the bottom part showing the almost symmetrical patterns of flattened waves with the number of 1.5, 2.0 and 3.0 respectively. A hydro code Autodyn 2D was adopted to simulate the experimental phenomena generated in this explosive driven impact test system for cylinders. The numerical results reproduced experimental final lengths and deformation patterns of impacted cylinders successfully for three cases. The numerical time-histories of momentum for the flyer plates and axial stresses at the sectional surface in the bottom support plate indicated the momentum absorption ratios of 22 – 31 %.

Keywords: Dynamic axial buckling, Stainless steel cylinder, Explosive driven flyer, Symmetrically deformed fold, Momentum absorption ratio.

1. Introduction

The knowledge of dynamic deformation and failure responses of structural components is of great importance in fracture control and safety evaluation for accidental impact of vehicles and crashworthiness shielding, blast of high-energy storage containers and space applications. The buckling behavior¹⁾ of a circular cylindrical shell, one of the most popular structural components has been studied and the unique progressive axisymmetric plastic buckling phenomena²⁾ with sequential folds had been introduced for some combinations of configurations and material characteristics of cylinders. Recently the transient deformation behavior and energy absorption of axially impacted circular tubes have been investigated experimentally³⁾ and numerically⁴⁾ for the fundamental evaluation database of vehicle crashes, where the cylinders are impacted against large amount of weight or rigid wall with a low velocity range of automobile speed.

In this study, steel cylinders were axially impacted by the

flyer plates of the same material in considering of shell structures with a high velocity range of trains, aircrafts or fragments of exploding vessels. The flyer plates were driven by the plane detonation wave generator of PETN (pentaerythritoltetranitrate) developed^{5), 6)} using wire explosion techniques. Numerical simulations of experimental procedures for cylinders impacted by explosively driven plates were performed using a two-dimensional analysis code for shock problems, Autodyn-2D. The calculations are compared to the test results with respect to deformed shapes, and the momentum absorption ratios are examined from the impact stress history.

2. Experimental procedure

Experiments are performed utilizing the explosion test facilities at the Shock Wave and Condensed Matter Research Center, Kumamoto University.

Figure 1 shows the explosive driver system for circular flyer plate (diameter, height, mass: 80, 20 mm, 2.0 kg)

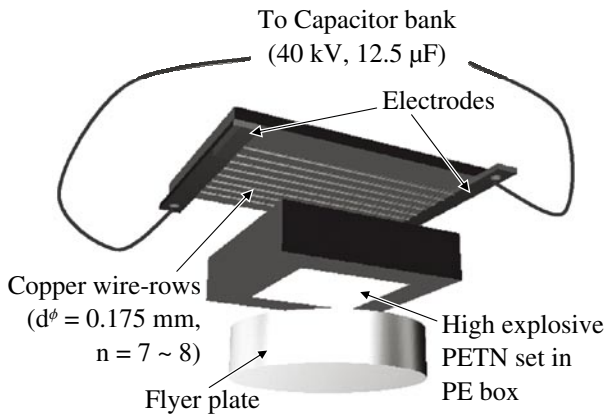


Fig. 1 Explosive driver system for circular flyer plate using wire-row explosion techniques.

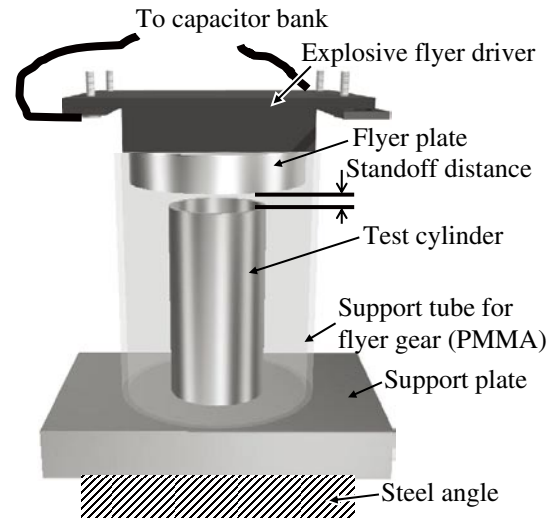


Fig. 2 Dynamic buckling test assembly for cylinders impacted by explosively driven flyer plate.

Table 1 Dimensions and materials for components of test assembly.

Components	Materials	Sizes (mm)	Other contents
Explosive (Flyer driver)	PETN	$50 \square \times H$ ($H = 10, 15, 20$)	Charged density (powder): $0.93-0.95 \text{ g} \cdot \text{cm}^{-3}$ Gurney energy: $2.93 \text{ J} \cdot \text{kg}^{-1}$
Flyer plate	JIS SUS304 steel	$D^\phi \times t$ ($= 80 \times 20$)	Mass: 800 g Standoff distance: 10 mm
Test cylinder	JIS SUS304 steel	$D_o^\phi \times t \times L$ ($= 34 \times 1.65 \times 100$)	Yield stress: $> 205 \text{ MPa}$ Tensile strength: $> 520 \text{ MPa}$
Support plate	JIS 4340 steel	$L \square \times t$ ($= 130 \times 20$)	(Placed on a steel angle)
Support tube for flyer gear	PMMA	$D_o^\phi \times t \times L$ ($= 34 \times 1.65 \times 100$)	(Transparent)

of 18Cr-8Ni stainless steel, JIS SUS304 using wire-row explosion techniques, which was basically developed for spall tests⁶⁾ and in this study applied to a flyer drive system modifying plate dimensions. In this system, slab-like installed powder PETN (density: $0.90-0.95 \times 10^3 \text{ kg} \cdot \text{m}^{-3}$, volume: $50 \times 50 \times H \text{ mm}$) is initiated by the simultaneous explosion of parallel copper wire rows (wire diameter: 175 μm , the ratio of PETN thickness of wire interval: 1.3-1.5) placed over the entire outer surface using an impulsive discharge current from a capacitor bank of 40 μF , 20 kV, producing a planar detonation front in the PETN layer immediately after the initial explosion. The detonation wave transfers a one-dimensional triangular pressure pulse into the flyer plate and generates small amount of spall damages inside the plate by the interaction of expansion waves emerged due to the reflection of strong shock waves at the free surface and other strong expansion wave coming from behind the detonation wave before the acceleration of the plate, and the plate was replaced by new one for every test.

The dynamic buckling test assembly for cylinder specimens (length, outer diameter, thickness: 100, 34, 3 mm) of SUS 304 is shown in Fig. 2 where the explosive driver system is located at the upper part and the standoff dis-

tance from the downward flyer plate to the cylinder specimen is adjusted 10 mm and the impact velocities are changed by the PETN height of H: 10, 15 and 20 mm. Dimensions and materials for the components of this test assembly are summarized in Table 1.

3. Numerical time histories of impact velocity and momentum for flyer plates

Some optical measurements for the velocity of flyer plate were performed excluding the influence of impulse current but they did not produce sufficiently reliable data because of the blowout of detonation gas preceding the flyer plate. In this study, impact velocities are numerically estimated at first and the calculated values are evaluated afterward from the comparison of numerical and experimental deformation behavior.

Figure 3 shows two dimensional axisymmetric finite difference model of test assembly for cylinders impacted by explosively driven flyer plate and a table including equation of state models and stress-strain relations⁷⁾ in the library of the hydro code, Autodyn 2D, used in this study. The wall thickness was divided into three layers and the displacement of x direction at the bottom surface of the plate is restrained. A squarely installed PETN is assumed

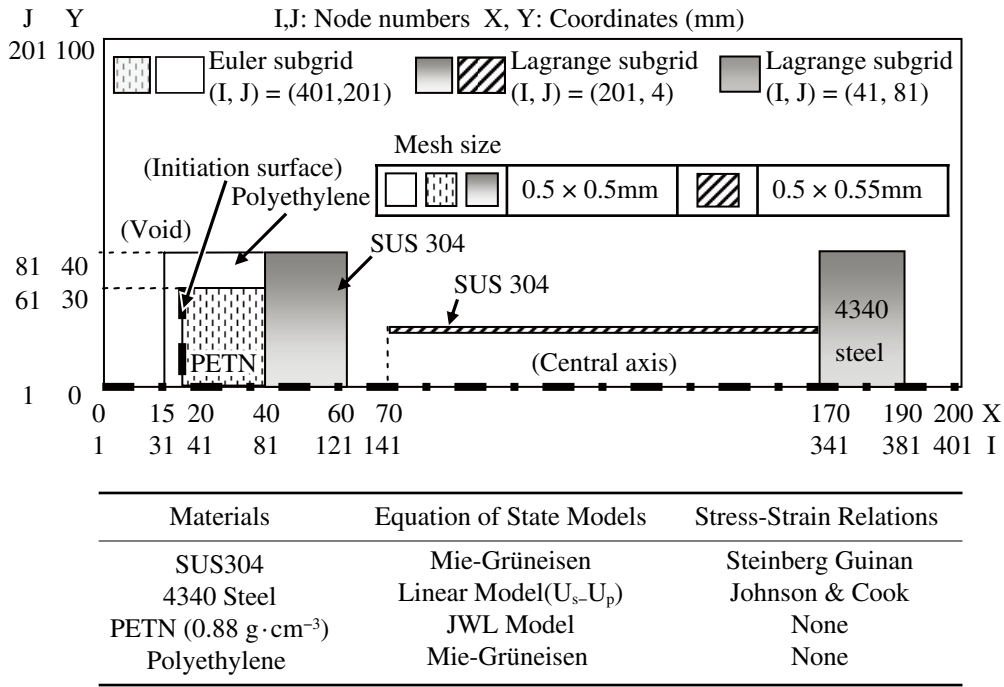


Fig. 3 Two dimensional axisymmetric finite difference model of test assembly for cylinders impacted by explosively driven flyer plate a table including equation of state models and stress-strain relations in the library of the hydro code, Autodyn 2D. The displacement of x direction at the bottom surface of the support plate is restrained.

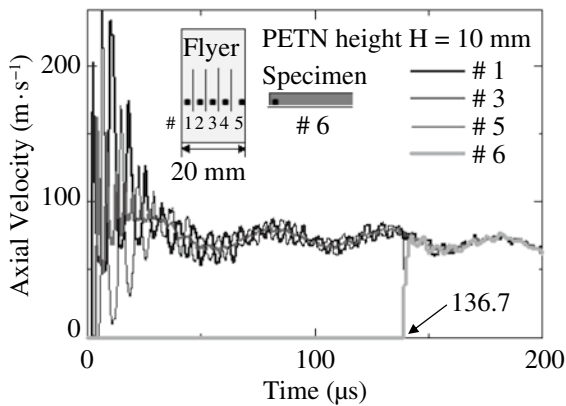


Fig. 4 Typical numerical time histories of axial velocities at the locations in the flyer plate and the edge of the cylinder for the case of PETN height $H = 10 \text{ mm}$. In this case, the impact velocity is $79.5 \text{ m} \cdot \text{s}^{-1}$ at $136.7 \text{ } \mu\text{s}$.

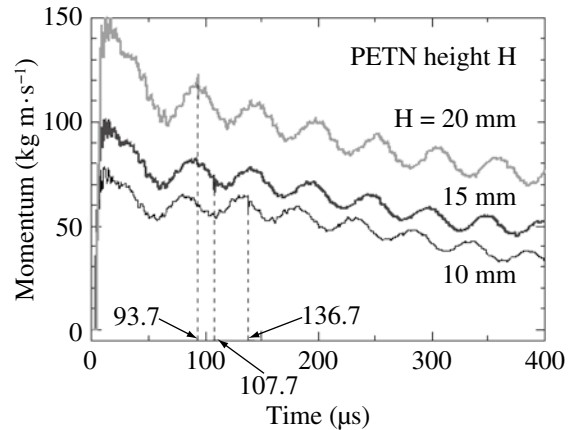


Fig. 5 Numerical time histories of average values of axial momentum at the representative three locations of flyer plates as shown in the former figure for the three cases of PETN height H 10, 15 and 20 mm with the impact times

to be a circular plate of equivalent volume. The experimental results introduced in next chapter indicate that two dimensional analyses in this study are practically effective for the understanding of the phenomena.

The flyer plate impacts on the upper edge of the cylinder specimen pulsating due to internal oscillation of stress waves produced by detonation wave.

Figure 4 represents typical numerical time histories of axial velocities at the locations in the flyer plate and the edge of the cylinder for the case of PETN height H : 10 mm. In this case, the impact velocity V_i is $79.5 \text{ m} \cdot \text{s}^{-1}$ at $136.7 \text{ } \mu\text{s}$, which is an elapsed period from the numerical PETN initiation. Other numerical impact velocities were

91.6 and $119.9 \text{ m} \cdot \text{s}^{-1}$ for H : 15 and 20 mm. Similarly axial momentum values M_F were numerically obtained as average values at the representative three locations # 1, 3 and 5 in flyer plates shown in the former figure.

Figure 5 shows time histories of the flyer momentum for three cases of PETN heights, where the impact times and corresponding momentum values are designated. Numerical velocities V_i and momentum values M_F of flyer plates at the impact to test cylinders are summarized as shown in Table 2 for tested three cases.

Gurney velocities⁸⁾ calculated using the estimated Gurney energy of $2.93 \text{ J} \cdot \text{kg}^{-1}$ are also shown as reference showing considerable correspondences.

Table 2 Numerical velocities V_I and momentum values M_F of flyer plates at the impact to test cylinders for three test cases. Gurney velocities V_G are also shown as reference.

Explosive height H (mm)	10	15	20
Impact velocity V_I ($\text{m}\cdot\text{s}^{-1}$)	79.5	91.6	119.9
Impact momentum M_F ($\text{kg}\cdot\text{m}\cdot\text{s}^{-1}$)	63.6	73.3	95.9
(Ref.) Gurney velocity V_G ($\text{m}\cdot\text{s}^{-1}$)	79.3	107.9	135.2

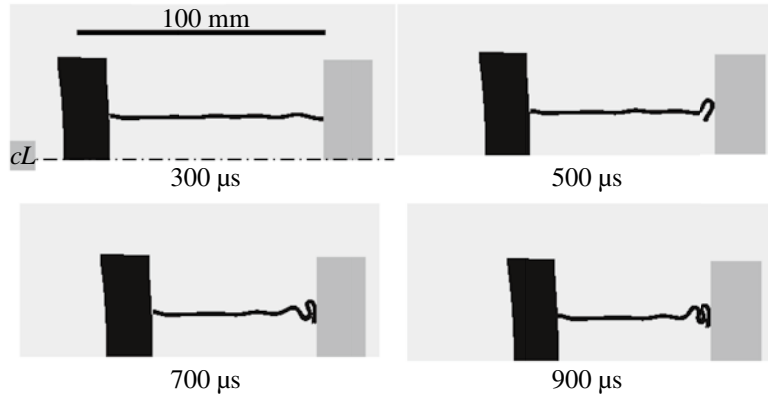


Fig. 6 Typical numerical progressive axisymmetric plastic buckling phenomena with sequential folds for the case of PETN height H : 15 mm. The time is the elapsed period from the numerical PETN initiation.

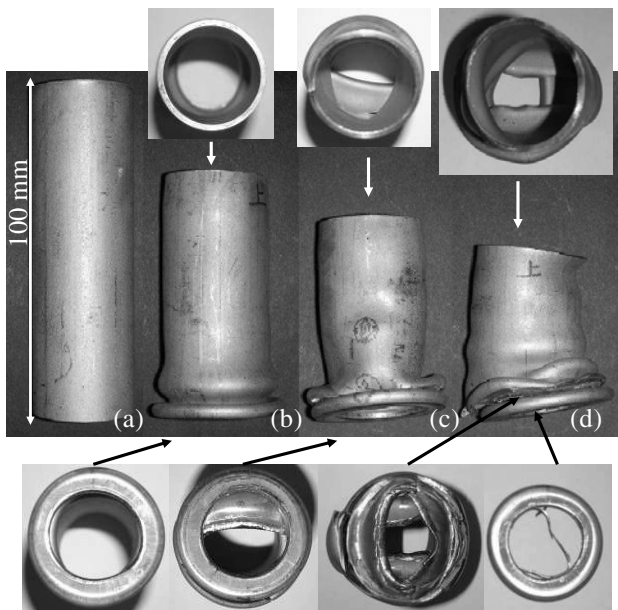


Fig. 7 Photos of (a) an initial test cylinder and plastically buckled cylinders due to axial impact of flyer plates driven by high explosive PETN with the height H of (b) 10 mm, (c) 15 mm and (d) 20 mm. View photos from the top and bottom of the buckled cylinders are also shown additionally.

4. Experimental and numerical progressive plastic buckling phenomena for cylinders

Numerical simulations has indicated that the circular flyer plate deforms like a shallow pan at the impact and the compressive axial stress wave generated at the upper edge travels through the cylinder in around $20 \mu\text{s}$ to the bottom followed by subsequent complicated stress oscillations reducing their amplitudes and final appearances of bending stresses and nodes for folding and flattening.

Typical numerical progressive axisymmetric plastic buckling phenomena with sequential two folds and final shrunken length of 60.4 mm are represented in Fig. 6 for the case of PETN height H : 15 mm. In cases of H : 10 and 20 mm, test cylinders buckled similarly leaving the deformed shapes with final length of 75.2 and 49.1 mm and the number of folds of 1.5 and 3.0 respectively.

Figure 7 shows photos of (a) an initial test cylinder and plastically buckled cylinders due to axial impacts of flyer plates driven by high explosive PETN with the height H of (b) 10 mm, (c) 15 mm and (d) 20 mm. View photos from the top and bottom of the buckled cylinders are also shown additionally, where the first flattened ring is separated from the bottom part for the case of H : 20 mm. Such experimentally deformed shapes of cylinders are basically axisymmetric and they correspond to those of the two dimensional numerical results except that non-axisymmetric oval and triangle shaped modes partially appear for the cylinders with higher impact velocities. The oval shape of the upper edge and non-axisymmetric deformation for the cylinder in case of H : 20 mm suggest that the influence of the imperfection or non-simultaneity of flyer impact becomes notable for the stronger hit of flyer. The recovered flyer plates were deformed as numerical simulations predicted and obvious spall damages were recognized for H : 20 mm. The final average lengths and fold numbers of tested cylinders also coincide with those of numerical results as shown in Fig. 8 (a) and (b) indicating practical validity of two dimensional numerical simulations in this study.

The numerical final shrunken lengths were defined as those of cylinders at the times: 848, 999 and $1066 \mu\text{s}$ when the average velocities of # 1 – # 5 locations shown in the Fig. 4 diminished and reached zero or negative first for three cases of H : 10, 15 and 20 mm respectively.

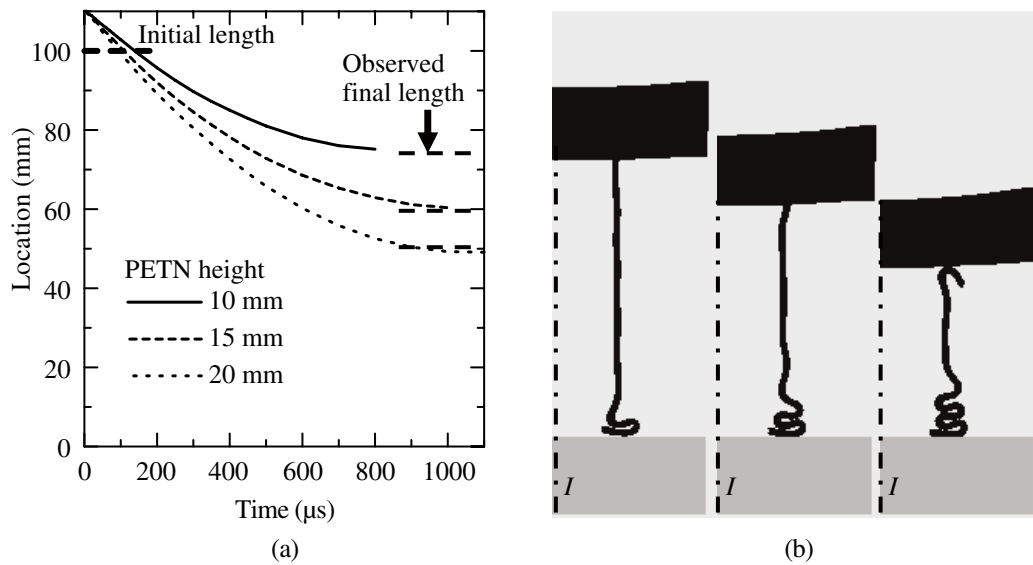


Fig. 8 (a) Numerical time-histories of explosive-driven flyer locations or shrinkage phenomena of progressively buckled cylinders for PETN height H 10, 15 and 20 mm with observed average lengths of buckled cylinders, and (b) corresponding numerical final profiles of deformed cylinders.

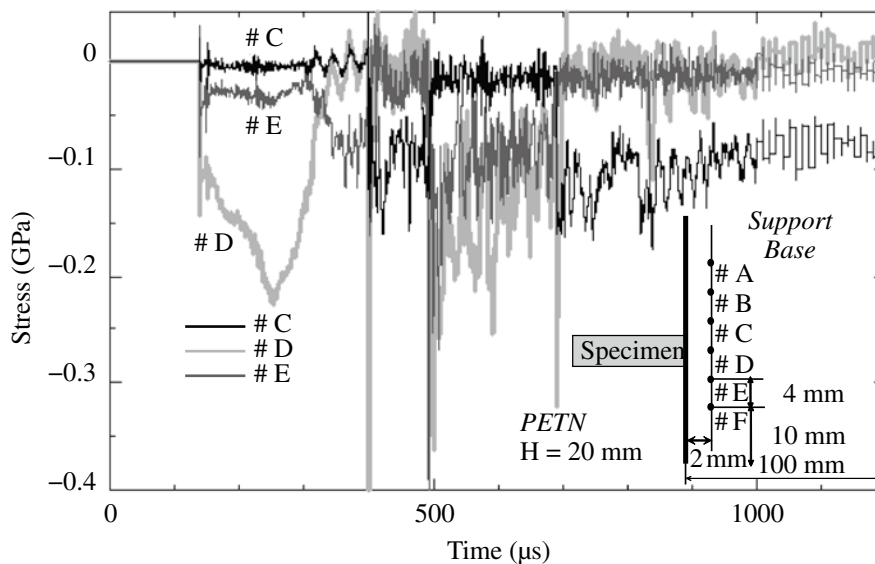


Fig. 9 Typical numerical time-histories of axial stresses at the representative three points on 2 mm depth layer from the surface in the support plate for the case of PETN height H : 20 mm.

5. Discussions and Conclusions

Dynamic buckling phenomena for 304 stainless steel cylinders impacted by explosively driven flyer plates were experimentally obtained and they have been successfully understood with the help of practical axisymmetric numerical simulations. Finally momentum values absorbed by the cylinder deformation are numerically investigated calculating the approximate impulse values I_M passing through the layer in the support plate from the axial stress - time diagrams at the six locations or concentric circles spacing 4 mm from the central axis of the plate. The end of time integration is the same time as defined for final numerical cylinder length in every case. In this calculation, the support plate is assumed thick (100 mm) in order to attenuate the reflected stress waves from the bottom surface.

Figure 9 shows typical numerical time-histories of axial

stresses at the representative three points on 2 mm depth layer from the surface in the support plate for the case of PETN height H : 20 mm. It is seen that the progressive plastic buckling phenomena with sequential folds accompany very complex stress oscillations in the support plate. The impulse value I_M of $72.2 \text{ kg}\cdot\text{m}\cdot\text{s}^{-1}$ or an absorbed momentum value $M_F - I_M$ of $21.0 \text{ kg}\cdot\text{m}\cdot\text{s}^{-1}$ was approximately obtained from the time integration of stress histories. The momentum absorption ratio $(M_F - I_M) / M_F$ of 21.9 % is not so large but it is known that the progressive deformation of the impacted cylinder has effectively moderated the steep shock loading produced by the flyer impact.

Table 3 summarizes experimental and numerical final lengths L_E , L_C of the buckled cylinders, the numbers N_E , N_C of wavy deformed and flattened symmetrical folds,

Table 3 Summary of experimental and calculated final lengths L_E , L_C of the buckled cylinders, the numbers N_E , N_C of wavyly deformed and flattened folds, and numerical momentum values $M_F - I_M$ absorbed by cylinder buckling deformation and momentum absorption ratios $(M_F - I_M) / M_F$.

Explosive height H (mm)	10	15	20
Experimental final cylinder length L_E (mm)	73.5	59.6	50.3
Calculated final cylinder length L_C (mm)	75.2	60.4	49.1
Number of observed final folds in cylinder N_E	1.5	2.0	3.0
Number of calculated final folds in cylinder N_C	1.5	2.0	3.0
Cal. absorbed momentum $M_F - I_M$ ($\text{kg} \cdot \text{m} \cdot \text{s}^{-1}$)	13.7	22.7	21.0
Momentum absorption ratios $(M_F - I_M) / M_F$ (%)	21.5	31.0	21.9

and numerical momentum values $M_F - I_M$ absorbed by cylinder buckling deformation and momentum absorption ratios: $(M_F - I_M) / M_F$. Calculated absorbed momentum values are almost same for the case of H : 15 and 20 mm. It possibly comes from inaccuracy due to complicated stress oscillations in the support plate.

In this study, steel cylinders of SUS 304 were axially impacted by the explosively driven flyer plates with variation of three explosive heights using wire-row explosion techniques and they were almost axisymmetrically buckled generating plastically deformed folds mainly at the bottom sides. Two dimensional numerical simulations reproduced experimental deformed shapes, fold numbers and shrunken length of the cylinders successfully, indicating the impact velocities of $79.5 - 119.9 \text{ m} \cdot \text{s}^{-1}$ and momentum absorption ratios of $21.5 - 31.0 \%$.

Additional flyer impact tests of cylinders with extended configurations and loads are to be continued for non-axisymmetric buckling conditions and more effective energy absorption.

References

- 1) S. P. Timoshenko and J. M. Gere, "Theory of Elastic Stability", pp. 457-461 (1961), McGraw-Hill.
- 2) J. W. Geckeler, Z. Angew. Math. U. Mech., 8,341 (1928).
- 3) Y. Akahoshi, S. Gotanda, T. Koura and Y. Okada, 59th Annual Meeting of JSME Kyushu Branch, No. 068-1, pp. 35-36 (2006), Fukuoka.
- 4) S. Haruyama, M. Takano, K. Ushijima and D. Chen, Transactions of the Japan Society of Mechanical Engineers. A, 71, 1030 (2005).
- 5) T. Hiroe, H. Matsuo, K. Fujiwara, M. Yoshida, S. Fujiwara, M. Miyata, S. Sakai, T. Fukano and T. Abe, Sci. Tech. Energetic Materials, 57, 49 (1996).
- 6) T. Hiroe, K. Fujiwara, H. Matsuo and N. N. Thadhani, Fourth International Symposium on Impact Engineering, pp. 851-856 (2001), Kumamoto.
- 7) D. J. Steinberg, S. G. Cochran, and M. W. Guinan, J. Appl. Phys., 51, 1498 (1980).
- 8) R. Gurney, Report No. 405, Ballistic Research Laboratory, (1943).

爆発飛翔板の衝突による304ステンレス鋼円筒の動的座屈に関する実験と数値解析

廣江哲幸[†], 藤原和人, 波多英寛, 佐嶋圭介

本研究では、鋼鉄板上に垂直に設置した18Cr-8Niステンレス鋼製円筒(軸長100 mm, 外形34 mm, 肉厚3 mm)に、上方から同材の飛翔円板(直径80 mm, 厚さ20 mm)を軸方向に高速衝突させた。衝突円板は、上面に設置した粉末状PETN爆薬(密度 $0.90 - 0.95 \times 10^3 \text{ kg} \cdot \text{m}^{-3}$, 薬厚10, 15, 20 mm)の自由表面に平行銅細線を配し衝撃大電流で一斉爆発させて生成させた平面爆轟ガスによって飛翔させた。

供試円筒には、薬厚量に応じて約80, 92, 120 $\text{m} \cdot \text{s}^{-1}$ の推定速度で円板が衝突し、いずれも円筒の支持端側で軸対象波型の塑性座屈変形が生じており、その折畳み波数は各々1.5, 2.0, 3.0であった。また衝撃解析コードAutodyn 2Dを用いて本研究の爆薬駆動円筒衝撃試験システムでの実験現象について数値シミュレーションを行った。その数値解析結果は、円板衝突実験による円筒の全体収縮変形量や折畳パターンを良好に再現していた。そして飛翔板の運動量と円筒支持板内の断面を通過する軸方向応力の時間履歴解析から本研究における円筒の運動量吸収率が22-31%であることが分かった。

*熊本大学大学院自然科学研究科機械システム工学部門 〒860-8555 熊本市黒髪2-39-1

[†]Corresponding address: hiroe@gpo.kumamoto-u.ac.jp